Available online at www.sciencedirect.com
SCIENCE DIRECT®
ELSEVIER
Journal of Magnetism and Magnetic Materials 301 (2006) 452–457
Journal of magnetism and magnetic materials
www.elsevier.com/locate/jmmm

Crystal structure and some transport properties of Na-doped $LaMnO_y$

A.M. Ahmed*, S.A. Saleh, E.M.M. Ibrahim, H.F. Mohamed

Physics Department, Faculty of Science, South Valley University, 82524 Sohag, Egypt

Received 1 May 2005
Available online 19 August 2005

Abstract

The crystal structure, electrical resistivity (ρ), magnetoresistance (MR) and Seebeck coefficient (S) of $La_{1-x}Na_xMnO_y$ ($x = 0.075$, 0.1, 0.125,0.15, and 0.175 at%) are investigated. $La_{1-x}Na_xMnO_y$ crystallizes in a single-phase rhombohedral structure. The temperature dependence of the resistivity with and without magnetic field shows a metal–semiconductor transition at T_m, which depends on the Na content. We determine the activation energy E_ρ in the semiconductor region. The magnetoresistance MR has a negative sign. The sign of S changes from positive to negative as T increases and S becomes more negative at high concentrations of Na doping.

PACS: 75.30.V; 72.15G; 72.20M

Keywords: Electrical resistivity; Magnetoresistance; Thermoelectric power

1. Introduction

Since the discovery of a colossal magnetoresistance (CMR) in perovskite manganese oxides $R_{1-x}A_xMnO_3$ (where R is a trivalent rare-earth element and A is a divalent metal elements such as Ca, Sr, Ba or Pb) much theoretical and experimental work has been done to investigate the physical properties and the application potential [1–6]. It has long been thought that the spin structure and the electronic transport properties of $R_{1-x}A_xMnO_3$ are correlated via the double-exchange (DE) mechanism [7] i.e, the hopping of e_g electrons between Mn^{3+} and Mn^{4+} ions mediated by oxygen anions.

So far most studies have focused on the divalent alkaline–earth–metal doping in $R_{1-x}A_xMnO_3$ compounds. In contrast, there are few reports on the study of monovalent alkaline–metal-doped samples [8–11]. Due to the difference in valence, alkaline –earth–metal doping and alkali–metal doping in $LaMnO_3$ can result in remarkably different consequences. In particular, it was reported that $R_yA_xMnO_3$ (A = Na, K and Rb) compounds

*Corresponding author. Tel./fax: +020 93 4602964/4601159.
E-mail address: Fikry_99@yahoo.com (A.M. Ahmed).

0304-8853/$ - see front matter © 2005 Elsevier B.V. All rights reserved.
doi:10.1016/j.jmmm.2005.07.021

crystallize in a rhombohedrally distorted perovskite structure without static Jahn-Teller deformation (space group $R\bar{3}c$) [12]. Therefore, the study of alkali–metal doping will offer a complementary understanding on the structure and electronic transport of doped $LaMnO_3$ crystals, which is significant for achieving a complete understanding of CMR effect in distorted perovskite manganates. Specifically, in this contribution we report on the crystal structure, magnetoresistance and thermoelectric power of sodium-doped $LaMnO_3$ compounds.

2. Experimental

Ceramic (polycrystalline) samples of $La_{1-x}Na_xMnO_y$ ($x = 0.075$, 0.1, 0.125, 0.15 and 0.175 at%) were prepared using the conventional solid-state reaction method. Stoichiometric amounts of La_2O_3, $Na_2CO_3.H_2O$ and $MnCO_3$ powders (all having 99.99% purity) were thoroughly mixed and then calcined for 24 h at 1000 °C and then quenched to room temperature. The powder thus obtained was then reground and pressed into pellets with a pressure of 7 ton cm^{-2} and subsequently sintered in air at 1100 °C for 10 h. The samples were examined by X-ray powder diffraction analysis which indicated the presence of single phase with perovskite-type structure. The XRD analysis was performed using Brucker (Axs-D8Advance) diffractometer at room temperature with Cu (Kα) radiation ($\lambda = 1.5406$ Å). The resistance was measured as a function of temperature using the standard four-probe method and air-drying conducting silver paste as in previous work [13]. The magnetoresistance (MR) ratio is defined by $MR = \Delta\rho/\rho_0 = (\rho_H - \rho_0)/\rho_0$, where ρ_H and ρ_0 are the resistivities with and without an applied magnetic field, respectively. The thermoelectric power measurements were carried using the sample two-heater method with copper electrodes as described in Ref. [13].

3. Results and discussion

Fig. 1 shows a typical X-ray diffraction a pattern for one of the $La_{1-x}Na_xMnO_y$ ($x = 0.075$, 0.1, 0.125, 0.15 and 0.175 at%) compounds. All samples are single phase with rhombohedral structure.

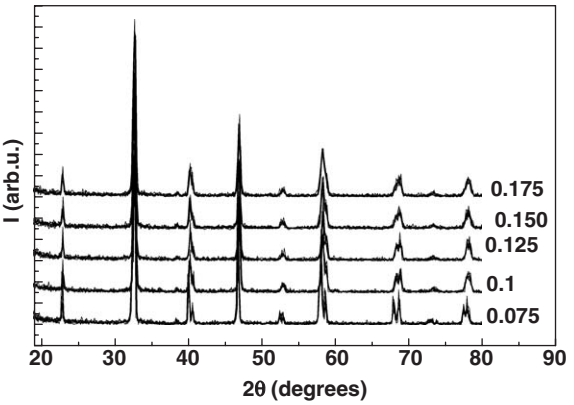

Fig. 1. X-ray diffraction pattern of $La_{1-x}Na_xMnO_y$.

The variation of the lattice parameters a and c with the concentration of Na in $La_{1-x}Na_xMnO_y$ ($0.07 \leqslant x \leqslant 0.175$ at%) are shown in Fig. 2(a). The lattice parameter a decreases with increasing Na concentration. Also, in general the c-parameter is inversely proportional with x. A similar feature is observed for the unit-cell volume as shown in Fig. 2(b), indicating that the lattice shrinks and the unit cell becomes smaller with increasing Na concentration. This is due to the smaller size of the Na^+ ion (113 pm) as compared to the La^{3+} ion (117.2 pm) [11].

Fig. 3 shows the variation of ρ with temperature for the five compositions at zero magnetic field. ρ (T) shows a peak at the metal–semiconductor (M–S) transition. These samples have a distinct metallic phase below the transition temperature (T_m) and above this temperature they become semiconducting. The M–S transition is believed to be correlated with the increase of the Mn–O–Mn bond angle [14]. On other hand, it was argued that PS-to-PM transitions correspond to a transition from a strong to weak electron–phonon coupling which gives rise to high resistivity, to a weak electron–phonon coupling that favours a low resistivity [15]. Therefore, it is reasonable to speculate that the $La_{1-x}Na_xMnO_y$ compounds, which crystallize in the rhombohedral perovskite structure, would be weaker phonon coupling as

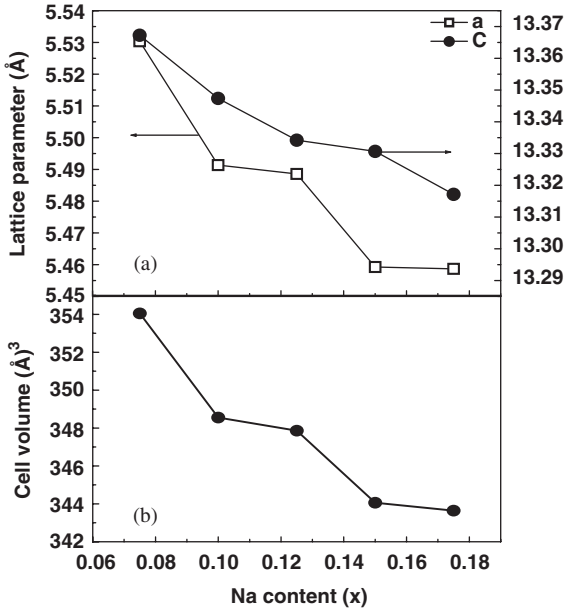

Fig. 2. (a) Lattice parameter a and c versus the Na content. (b) Variation of unit cell with the concentration of Na.

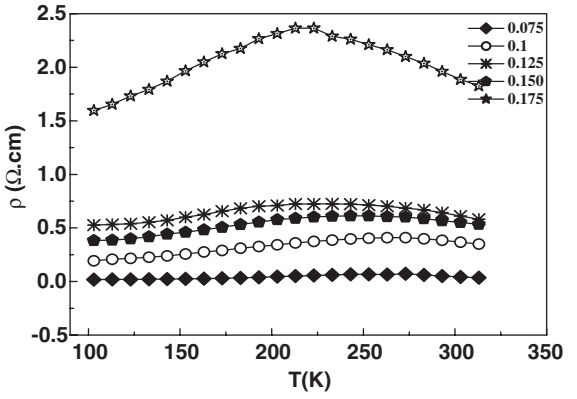

Fig. 3. The temperature dependence of the resistivity of $La_{1-x}Na_xMnO_y$ in zero field.

the sodium doping decreases. However, at high temperatures (above T_m) the activation energy, E_ρ, can be extracted from Eq. (1), (see in Table 1).

$$\rho = \rho_0 \exp(E_\rho / k_B T). \quad (1)$$

The values of E_ρ decrease with increasing Na content, in agreement with others [16–18].

The temperature dependence of the resistivity in zero applied field (ρ_0) and at 0.6 T ($\rho_{0.6}$) of the five samples are shown in Fig. 4. The resistivity shows a semiconducting behaviour above the metal–semiconductor transition temperature (T_m) for all cases. It can be seen from Fig. 4(a) that both ρ_0 and $\rho_{0.6}$ of $x = 0.075$ show two peaks, a sharp one at a higher temperature ($T_m = 273$ K) and a broad one at lower temperature ($T = 243$ K). The higher temperature peak just occurs at about T_c [8,10], indicating that it originates from the ferromagnetic–paramagnetic phase transition. The double exchange model can qualitatively explain this simultaneous electronic and magnetic transition. The second peak, which occurs at lower temperature, is surprising. Similar phenomena were observed by several groups [12,19–23], but there is still no generally accepted explanation though some hypotheses have been given.

Table 1
Values of E_ρ (eV) and T_m of $La_{1-x}Na_xMnO_y$

x at%	0.075	0.1	0.125	0.15	0.175
E_ρ (eV)	0.1414	0.0337	0.0170	0.0159	0.0181
T_m (K)	273	273	233	253	223

For $x \geqslant 0.1$ at%, only one peak is observed (T_m) which is a function of the Na concentration (see Figs. 4(b–e)). The semiconductor–metal transition (T_m), moves to a lower temperatures with the increment of the sodium concentration. The sodium will alter the Mn^{4+}/Mn^{3+} ratio which is one of the factors which determine the transport and magnetic properties of samples. In addition decrease in T_m with increase Na content (Table 1) can be interpreted as an increasing strength of the Mn–O–Mn bond with decreasing average A site ionic radius $\langle r_A \rangle$ due to the partial substitution of smaller Na^{1+} ions for larger La^{3+} ions. This substitution causes a narrowing of the bandwidth, thus decreasing of, e.g., electrons which in turn results in a weakening of the double exchange interaction magnetism [24].

The negative magnetoresistance, MR% was calculated from the ρ–T relation at zero and applied magnetic field (0.6 T).

$$MR = (\rho_H - \rho_0)/\rho_0. \quad (2)$$

Figs. 5(a–e) show the temperature dependence of the magnetoresistance of $La_{1-x}Na_xMnO_y$. For

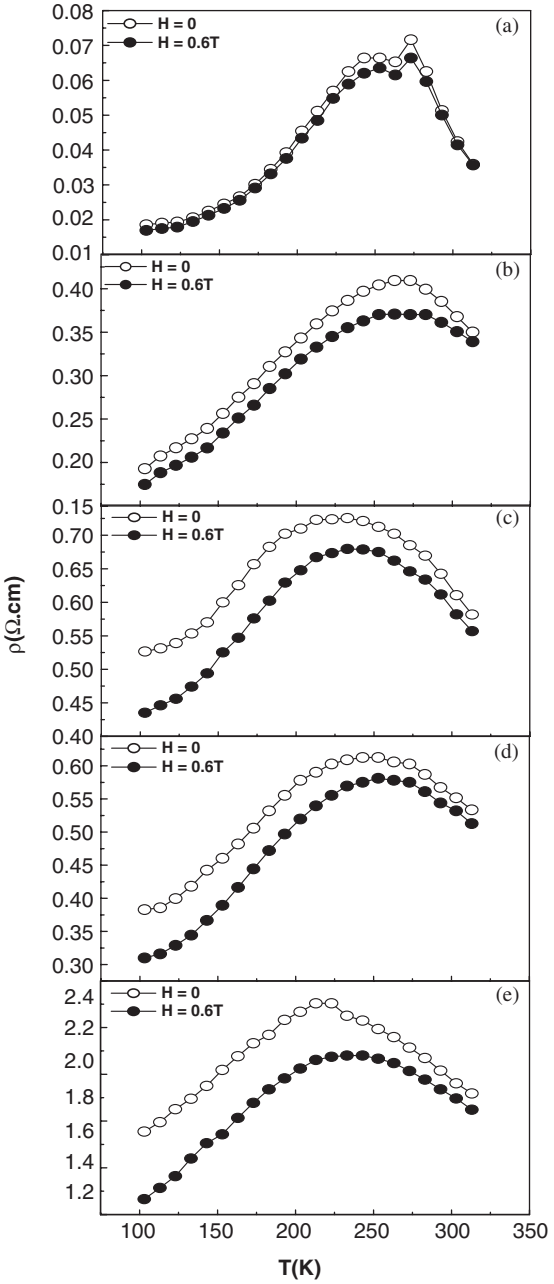

Fig. 4. ρ vs. T for H = 0 and 0.6 T for $La_{1-x}Na_xMnO_y$, $a-x=0.075$, $b-x=0.1$, $c-x=0.125$, $d-x=0.150$ and $e-x=0.175$ at%.

the lowest Na concentration, the MR% shows many peaks, two peaks agree with ρ–T curve (243 K and T_m). On the other hand, the MR is highest at low temperature. For $x=0.1$, MR shows a high value at T_m and at low temperatures. In addition, for the Na $\geqslant$ 0.125 at%, the MR shows a small peak about T_m. As in Fig. 5, the large MR around T_m mainly originates from the intrinsic CMR, while the large MR at lower temperature probably comes from spin-dependent transport across grain boundaries [25–27].

Figs. 6(a)–(e) show the temperature dependence of the thermoelectric power for $x=0.075$, 0.1, 0.125, 0.15 and 0.175 at%, respectively. The values of S for the five samples are small (in the microvolt range). As it is seen in Fig. 6(a), S shows two peaks at $T=125$ and 265 K, the second peak agrees with the M–S transition T_m. On the other hand, the sign of S changes from positive to negative at high temperatures. This agrees with the divalent doping in $LaMnO_3$ [28–30]. Figs. 6(b–e) show the same behaviour, S increases with T and then decreases (show a peak about 175 K). On the other side, the sign of S is negative and becomes more negative with increasing x, except for the highest Na-content. The observation that S becomes more negative while formally the hole-content increases observed in the high T_c cuprates. For $La_{1-x}Sr_xCoO_3$ system [31] also the thermopower shows the same trend. It is possible that the observed dependence of S of $La_{1-x}Sr_xCoO_3$ [31] shows the same trend, content is generic in materials with strong hybridization of oxygen p and transition metal d bands with a component of a charge transfer between the ligand and the cation.

Photoelectron spectroscopic studies [32] have shown the existence of both electron and hole-like bands below and above the Fermi level which are created via substitution. For the metallic samples the Fermi level lies in region where these two bands overlap. While the creation of Mn^{4+} in $LaMnO_3$ creates change in the hole-like band, creation of Mn^{3+} in $SrMnO_3$ or $CaMnO_3$ fills up the electron doped states. We can think of charge transport by both type of carriers (i.e., hole and electron) in the Na substituted $LaMnO_3$ systems. The observed total thermopower depends on the relative contribution of both type of carriers. The change in the sign of thermopower as a function of the Na content can thus be thought of as a

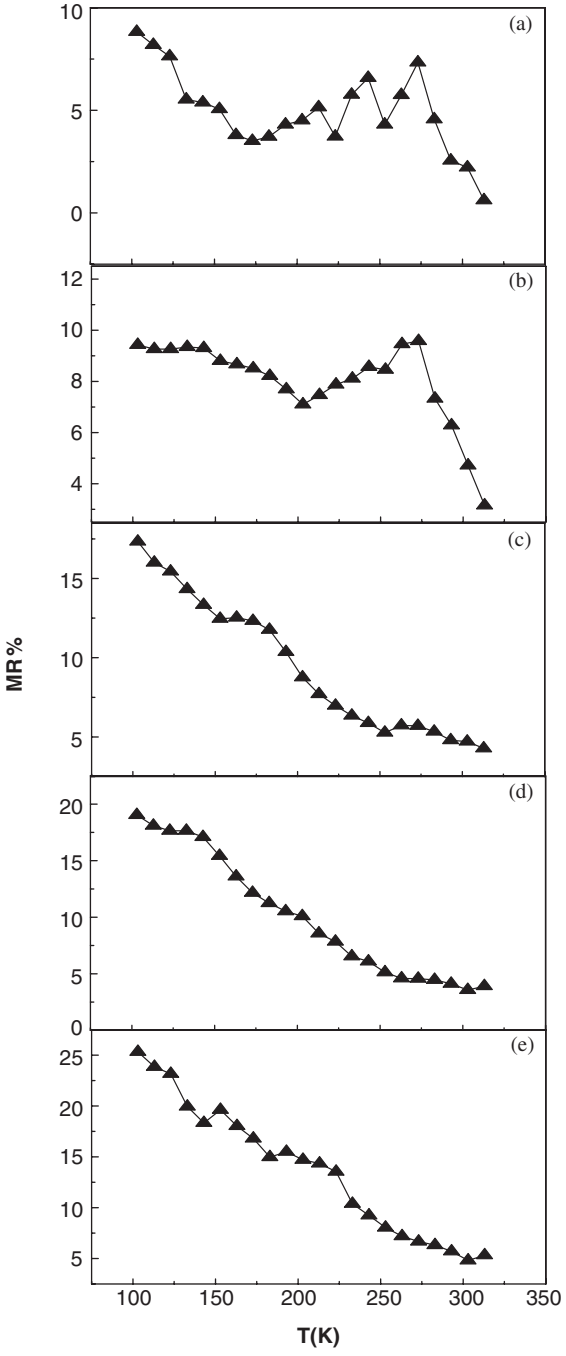

Fig. 5. The temperature dependence of MR% for samples at $H = 0.6$ T, $a - x = 0.075$, $b - x = 0.1$, $c - x = 0.125$, $d - x = 0.150$ and $e - x = 0.175$ at%.

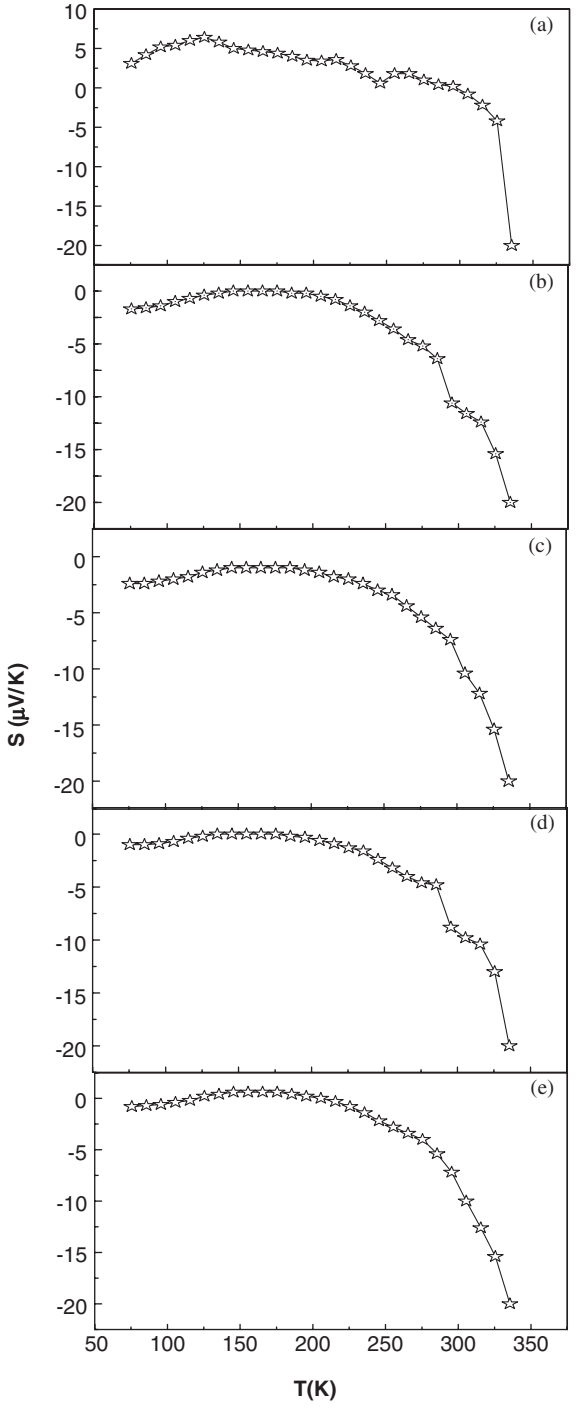

Fig. 6. The seebeck coefficient of the $La_{1-x}Na_xMnO_y$ system, $a - x = 0.075$, $b - x = 0.1$, $c - x = 0.125$, $d - x = 0.150$ and $e - x = 0.175$ at%.

crossover from hole-like carrier dominated region to an electron-like carrier dominated region.

4. Conclusion

In summary, the crystal structure, MR and thermoelectric power properties of $La_{1-x}Na_xMnO_y$ have been investigated systematically. The lattice parameters a and c and the unit cell volume decrease with an increase of the Na content. The resistivity curves show a metal–semiconductor transition for all samples. The M–S transition temperature decreases with increasing Na content. This is due to the partial substitution of smaller Na^{1+} ions for larger La^{3+} ions or due to Zener bond blocking.

Our thermoelectric power data show the signature of both hole and electron type carriers depending on the temperature as well as the Na content. Such a behaviour, however, is expected given the electronic structure of these oxides.

Acknowledgments

We would like to thank Prof. Dr. K. Bärner (Goettingin university, Germany) for many helpful discussions and Prof. Dr. M. M. Ibrahim for continuous encouragement.

References

[1] R. von Helmolt, J. Wecker, B. Holzapfel, L. Schultz, K. Samwer, Phys. Rev. Lett. 71 (1993) 2331.
[2] J.M.D. Coey, M. Viret, S. von Molnar, Adv. Phys. 48 (1999) 167.
[3] I. El-Kassab, A.M. Ahmed, P. Mandal, K. Bärner, A. Kattwinkel, U. Sondermann, Physica B 305 (2001) 233.
[4] A.M. Ahmed, A. Kattwinkel, K. Bärner, C.P. Yang, J.R. Sun, G.H. Rao, Physica B 324 (2002) 102.
[5] A.M. Ahmed, M. Boshta, R. Braunstein, V. Morchshakov, K. Bärner, C.P. Yang, J.R. Sun, G.H. Rao, J. Alloys Compounds 348 (2003) 23.
[6] A.M. Ahmed, V. Morchshakov, K. Bärner, C.P. Yang, P. Terzieff, H. Schickitanz, T. Gron, J.R. Sun, G.H. Rao, Phys. Status Solidi (a) 200 (2) (2003) 407.
[7] C. Zener, Phys. Rev. 82 (1951) 403.
[8] G.H. Rao, J.R. Sun, K. Bärner, N. Hamad, J. Phys. Condens. Matter 11 (1999) 1528.
[9] S.L. Ye, W.H. Song, J.M. Dai, K.Y. Wang, S.G. Wang, J.J. Du, Y.P. Sun, J. Fang, J.L. Chen, B.J. Gao, J. Appl. Phys. 90 (6) (2001) 2943.
[10] Z.Q. Li, E.Y. Jiang, D.X. Zhang, D.L. Hou, W.C. Li, H.L. Bai, Phys. Lett. A 277 (2000) 56.
[11] S. Roy, Y.Q. Guo, S. Venkatesh, N. Ali, J. Phys., Condens. Matter 13 (2001) 9547.
[12] T. Shimura, T. Hayashi, Y. Inaguma, M. Itoh, J. Solid State Chem. 124 (1996) 250.
[13] A.M. Ahmed, Physica B 352 (2004) 330.
[14] J.B. Torrance, P. Lacorre, A.I. Nazzal, Phys. Rev. B 45 (1992) 8209.
[15] A.J. Millis, B.I. Shraiman, R. Mueller, Phys. Rev. Lett. 77 (1996) 175.
[16] R.M. Kusters, J. Singleton, D.A. Keen, R. McGreevy, W. Hayes, Physica B 155 (1989) 362.
[17] G.C. Xiong, S. Bhagat, Q. Li, M. Dominguez, H. Ju, R. Greene, T. Venkatesan, Solid State Commun. 97 (1996) 599.
[18] M.F. Hundley, M. Hawley, R.H. Heffner, Q.X. Jia, J.J. Neumeier, J. Tesmer, Appl. Phys. Lett. 67 (1995) 860.
[19] M. Itoh, T. Shimura, J. Ding Yu, T. Hayashi, Y. Inaguma, Phys. Rev. B 52 (1995) 12522.
[20] X.L. Wang, S.J. Kennedy, P. Gehringer, W. Lang, H.K. Liu, S.X. Dou, J. Appl. Phys. 83 (1998) 7177.
[21] J.R. Sun, G.H. Rao, Y.Z. Zhang, Appl. Phys. Lett. 72 (1998) 3208.
[22] N. Zhang, W. Ding, W. Zhong, D.Y. Xing, Y. Du, Phys. Rev. B 56 (1997) 8138.
[23] R. Suryanarayanan, J. Berthon, I. Zelenay, B. Martinez, X. Obradors, S. Uma, E. Gmelin, J. Appl. Phys. 83 (1998) 5264.
[24] H.Y. Hwang, S.-W. Cheong, P.G. Radaelli, M. Marezio, B. Batlogg, Phys. Rev. Lett. 75 (1995) 914.
[25] A. Gupta, G.Q. Gong, G. Xiao, P. Lecoeur, P. Trouilloud, Y.Y. Wang, V.P. Dravid, J.Z. Sun, Phys. Rev. B 54 (1996) R15629.
[26] C. Dubourdieu, M. Audier, J.P. Senature, J. Pierre, J. Appl. Phys. 86 (1999) 6945.
[27] N.D. Mathur, G. Burnell, S.P. Isaac, T.J. Jackson, B.S. Teo, J.L.M. Driscoll, L.F. Cohen, J.E. Evetts, M.G. Blamire, Nature 387 (1997) 266.
[28] R. Mahendiran, S.K. Tiwary, A.K. Raychaudhuri, Phys. Rev. B 54 (1996) R9604.
[29] R. Mahendiran, S.K. Tiwary, A.K. Raychaudhuri, T.V. Ramakrishnan, R. Mahesh, N. Rangavittal, C.N.R. Rao, Phys. Rev. B 53 (1996) 3348.
[30] A. Asamitsu, Y. Moritomo, Y. Tokura, Phys. Rev. B 53 (1996) R2952.
[31] M.A. Senaris-Rondriguez, J.B. Goodenough, J. Solid State Chem. 118 (1995) 323.
[32] T. Saitoh, A.E. Bocquet, T. Mizokawa, H. Namatame, A. Fujimori, M. Abbate, Y. Takeda, M. Takano, Phys. Rev. B 51 (1995) 13942.